EUROPEAN JOURNAL OF PHYCOLOGY, 2021
https://doi.org/10.1080/09670262.2021.1966838

Taxonomic relationship between two small-sized *Chaetoceros* species (Bacillariophyta): *C. tenuissimus* and *C. salsugineus*, and comparison with *C. olympicus* sp. nov. from Catalan coastal waters (NW Mediterranean)

Laura Arin [a], Albert Reñé [a], Rachele Gallisai [a], Diana Sarno [b], Esther Garcés [a] and Marta Estrada [a]

[a]Institut de Ciències del Mar, CSIC, Pg. Marítim de la Barceloneta, 37–49, 08003 Barcelona, Spain; [b]Stazione Zoologica Anton Dohrn, Villa Comunale, 80121, Napoli, Italy

ABSTRACT

The majority of species of the highly diverse genus *Chaetoceros* are described as chain-forming, although several species are described as strictly solitary (such as *C. tenuissimus*) or having an alternate solitary and a chain-forming phase during their life history (such as *C. salsugineus*). In this study, the diversity of small forms of *Chaetoceros* from the NW Mediterranean coastal waters was explored through the morphological and molecular characterization of four different strains belonging to two distinct species. Based on their morphology, three of the strains were identified as *C. salsugineus* (Takano, 1983). The SSU and LSU rDNA sequences represented the first available for well-characterized *C. salsugineus* strains and were 96.6–100% similar to publicly available *C. tenuissimus* (Meunier, 1913) sequences. Both species share the same morphological features, such as setae and ultrastructure of the valves, as well as the rimoportula characteristics. In addition, the morphology of the solitary form of *C. salsugineus* matched with that of *C. tenuissimus*. Here, we propose the two species as synonyms (the name *C. tenuissimus* prevailing as it has priority for this taxon), emend the original description and designate an epitype. The fourth strain was identified as *C. olympicus* sp. nov., a new species, which alternates solitary and chain-forming forms within its life history. The main differential characteristics of this species are the absence of rimoportula both in terminal and intercalary valves, the setae ultrastructure, which is thin and circular in cross-section with a few, slightly twisted, rows of small rectangular poroids and some spirally arranged spines, and the morphology of the resting spores, with primary valve vaulted and covered with short to medium-sized spines, and secondary valve smaller, rounded and smooth. A comparison of *C. tenuissimus* and *C. olympicus* with other species as well as information on their life cycle and ecology is also provided.

HIGHLIGHTS

- Description of a new *Chaetoceros* species: *C. olympicus*.
- Proposal that *C. tenuissimus* and *C. salsugineus* are synonyms.
- Importance of morphological variability in life cycles for species identification.

ARTICLE HISTORY Received 5 March 2021; Revised 3 August 2021; Accepted 8 August 2021

KEYWORDS *Chaetoceros tenuissimus*; *Chaetoceros salsugineus*; ecology; life cycle; molecular; morphology; small-sized *Chaetoceros*

Introduction

Chaetoceros Ehrenberg is one of the most abundant and diverse diatom genera in the oceans (Rines & Hargraves, 1988; Malviya *et al.*, 2016; De Luca *et al.*, 2019*b*). Members of this genus are ecologically relevant since their contribution to the total primary production can be very important in many marine environments, especially in upwelling zones and coastal areas. The main characteristics of *Chaetoceros* are the presence of setae (siliceous projections) and the capacity to form chains. Some species are considered bloom-forming (Booth *et al.*, 2002; Trigueros *et al.*, 2002; Shevchenko & Orlova, 2010), while others, due to their morphological features or mucilage production, can be harmful for fish, causing mechanical damage and even death by clogging their gills (Horner *et al.*, 1997; Treasurer *et al.*, 2003).

About half of the approximately 400 described species (Hasle & Syvertsen, 1997) are taxonomically accepted (Guiry & Guiry, 2021). However, the actual number of species is difficult to determine because many of the descriptions were only based on light microscopy observations, lacking electron microscopy characterization, and without taking into account the intraspecific phenotypic variability and the morphological changes that may occur during the different phases of the life cycle of the organisms. In the last decades, the incorporation of molecular information into taxonomy pointed to intraspecific variability in *Chaetoceros* and discriminated cryptic or semi-cryptic species (see for example Degerlund *et al.*, 2012; Gaonkar *et al.*, 2017; Li *et al.*, 2017). In addition, molecular tools allowed the determination of the phylogenetic positions and systematic relationships within the

CONTACT Laura Arin larin@icm.csic.es; Albert Reñé albertrene@icm.csic.es; Rachele Gallisai gallisai@icm.csic.es; Diana Sarno diana.sarno@szn.it; Esther Gracés esther@icm.csic.es; Marta Estrada marta@icm.csic.es

This article was originally published with errors, which have now been corrected in the online version. Please see Correction (http://dx.doi.org/10.1080/09670262.2021.2000204)

Published online 12 Oct 2021

genus (Kooistra *et al.*, 2010; Gaonkar *et al.*, 2018; De Luca *et al.*, 2019*a*). Traditionally, *Chaetoceros* has been divided into three subgenera, *Chaetoceros* (formerly *Phaeoceros* Gran), *Hyalochaete* Gran and *Bacteriastroidea* Hernández-Becerril, and 22 sections (Ostenfeld, 1903; Hernández-Becerril, 1991, 1996; Hernández-Becerril & Flores Granados, 1998), although the classification in sections has been questioned for being based on morphological features and not on a natural grouping of species (Rines & Hargraves, 1988; Sar *et al.*, 2002). Based on multistate morphological characters, Rines & Theriot (2003) studied for the first time the evolutionary relationship of the Chaetocerotaceae family using a cladistic analysis and resolved that the genus *Chaetoceros* was paraphyletic, because it included *Bacteriastrum* species, and questioned the traditional classification of *Chaetoceros* in subgenera. Recently, De Luca *et al.* (2019*a*) also revealed the subgenus *Hyalochaete* as paraphyletic based on a multigene (nuclear, plastid and mitochondrial) phylogeny. Consequently, these authors rejected the *Chaetoceros* subdivision in subgenera and recognized some of the initial sections, one emended section and three new ones (one of them – section *Chaetoceros* – replacing the *Chaetoceros* subgenus).

The section *Simplicia* includes small-sized and fragile organisms, whose life form is generally as solitary cells or in pairs (Ostenfeld, 1903) but also able to form chains (De Luca *et al.*, 2019*a*). One of the species assigned to this section is *Chaetoceros tenuissimus*. This species was first described by Meunier (1913) from plankton samples off the North Sea as very small, solitary or paired cells provided with short setae arranged in the sagittal plane. Later descriptions determined that the setae emerged from the cell at an angle of 45° from both the apical and pervalvar axes (Rines & Hargraves, 1988; Hasle & Syvertsen, 1997; Sar *et al.*, 2002; Hoppenrath *et al.*, 2009; Baytut *et al.*, 2013; Bosak, 2013). Sar *et al.* (2002) provided a more accurate description of the species, including ultrastructural features, based on material from Atlantic coastal waters off Argentina. Recently, Gaonkar *et al.* (2018; see Supporting information S1) reported, for the first time, the formation of chains in several strains of *C. tenuissimus* and provided molecular information (18S and 28S rDNA sequences).

Takano (1983) described *Chaetoceros salsugineus* as small-sized and delicate organisms, from some brackish and estuarine waters of the Pacific coast of Japan, based on the observation of specimens frequently solitary or in short chains, and sometimes forming long chains. The author described three different forms: *C. salsugineus* f. *solitarius* (solitary form), *C salsugineus* f. *curtus* (chains of 3–4 cells) and *C. salsugineus* f. *salsugineus* (chains of 6–18 cells) and compared the morphology and ultrastructure of this species with those of other *Chaetoceros* taxa. Surprisingly, the high similarity of the solitary form with the species *C. tenuissimus* was not considered, although comparisons also included the solitary species *C. calcitrans* (Paulsen) Takano. However, the taxonomic history of this last species is intricate, as it underwent some taxonomic changes over time and several authors reported different synonymies. In particular, Rines & Hargraves (1988) and Hasle & Syvertsen (1997) considered it as a synonym of *C. tenuissimus*. Further studies focused on the morphology, ecology, growth rate and life cycle of *C. salsugineus* (Orlova & Selina, 1993; Orlova & Aizdaicher, 2000; Trigueros *et al.*, 2002; Shevchenko *et al.*, 2006; Ichimi *et al.*, 2012). The three forms of *C. salsugineus* were recognized as different stages in the development of this species in a natural environment (Orlova & Selina, 1993) and in culture (Orlova & Aizdaicher, 2000). *Chaetoceros salsugineus* was eventually assigned to section *Brevicatenata* Gran (small forms, chains straight, terminal setae thinner than other setae, one or two chloroplasts) by Orlova & Selina (1993). Trigueros *et al.* (2002) reported *C. salsugineus* for the first time in European waters (Urdaibai Estuary, North Spain) and compared the different forms with other small and delicate chain-forming or solitary species. They mentioned that the solitary form of *C. salsugineus* can easily be mistaken for *C. tenuissimus* and that differential characters could only be distinguished under TEM but did not specify which ones. Later, Bosak (2013) described the occurrence of *C. tenuissimus* and *C. salsugineus* in coastal waters of the Adriatic Sea and suggested that they could represent different morphological forms of the same species.

Knowledge of the diversity of small-sized and delicate *Chaetoceros* forms is hampered by the lack of proper identification. These species are usually misidentified because they cannot always be adequately separated from one another on a morphological basis under light microscopy, making it necessary to base their taxonomy on their ultramorphology and molecular information. As discussed elsewhere (Rines & Hargraves, 1988; Balzano *et al.*, 2017; De Luca *et al.*, 2019*a*), this problem is even more evident for small unicellular *Chaetoceros* taxa. Consequently, the aim of the present study is to characterize, using morphological and molecular information, the diversity of small-sized *Chaetoceros* organisms from the Catalan coast (NW Mediterranean Sea). We aim to clarify the taxonomic relationship between *C. tenuissimus* and *C. salsugineus*, and include the description of *C. olympicus*, a new species, which alternates solitary and chain-forming phases within its life cycle. Information on the life cycle and ecology of these species is also provided.

Materials and Methods

Sampling and analytical determinations

Four *Chaetoceros* strains were isolated from coastal waters off Barcelona and grown in culture.

Chaetoceros strains ICMB61 and ICMB64 were isolated in May 2016 and strain ICMB70 in February 2018 at station 1.4 (1.9 km from the coast, 40 m depth) (Table 1, Fig. 1) in the course of a time series of oceanographic variables and phytoplankton enumeration (among other parameters) carried out since 2002. The zone is located near the Olympic Harbour of Barcelona and receives the influence of the Besòs River and sporadically of four sewer overflows that can discharge important amounts of fresh water from rain runoff. Surface samples were taken with a bucket for strain isolation, salinity, inorganic nutrients and chlorophyll-*a* (Chl-*a*) determinations, and phytoplankton enumeration. In this work, we present data from February 2017 to May 2018. Details of the zone and of the sampling strategy can be found in Arin *et al.* (2013).

Strain ICMB72 was isolated from surface waters of station H, located at the mouth of the Olympic Harbour of Barcelona (Table 1, Fig. 1). Surface samples for temperature, salinity, inorganic nutrients, Chl-*a* and phytoplankton were obtained with a bucket with a weekly or biweekly frequency from March to May 2018.

At station 1.4, temperature data were taken from CTD casts and salinity was analysed with an AUTOSAL salinometer (OSIL, UK), and expressed using the practical salinity scale. At the harbour station those parameters were measured with a YSI 30 salinity, conductivity and temperature field sensor (Xylem Inc., USA). Inorganic nutrient samples were frozen prior to analysis. Soluble reactive phosphate, nitrate plus nitrite, nitrite, ammonium and silicate concentrations were analysed using the methods described in Grasshoff *et al.* (1999). Measurements were performed by Continuous Flow Analysis (CFA) on a Bran+Luebbe (currently SEAL) autoanalyser. Ammonium was measured by fluorometry. For Chl-*a* analysis, 100 ml of water were filtered thought Whatman GF/F fibre filters (25 mm diameter), which were subsequently frozen at −20°C until their further processing. Before analysis, the filters were placed in 90% acetone for ~24 h in the dark and at 4°C. The fluorescence of the extract was measured with a Turner-Designs fluorometer (Yentsch & Menzel, 1963). Phytoplankton samples were fixed with formol-hexamine to a final concentration of 0.4% (Throndsen, 1978) and organisms of sizes approximately >2 µm were

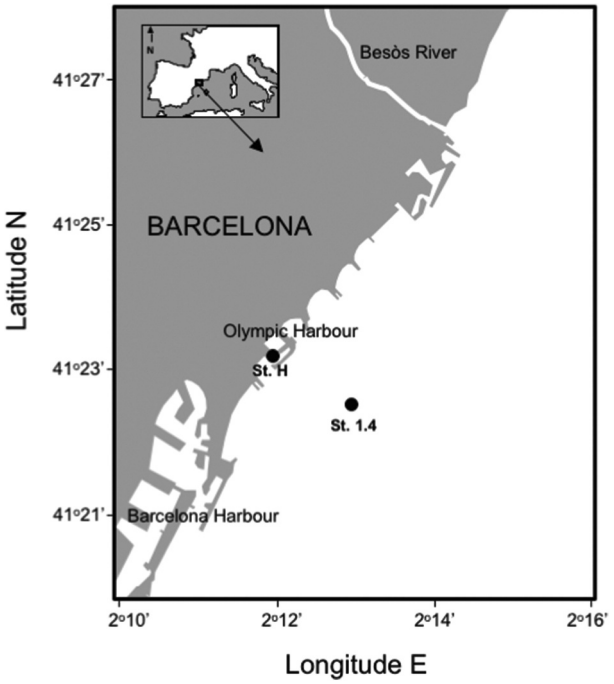

Fig. 1. Study area with the location of the sampling stations.

counted (from 50 ml settling chambers) using an inverted microscope (Utermöhl, 1958) at 200× and 400× magnification. Organisms were observed with bright field or phase contrast. Since February 2017, 500 ml of sample were also concentrated by a mesh of 20 µm for *in vivo Chaetoceros* spp. identification and enumeration. The volume of the concentrate was measured with a graduated tube (usually between 6–8 ml after washing the mesh with 0.2 µm of filtered seawater several times) and an aliquot was settled into a 3 ml sedimentation chamber and counted by the Utermöhl (1958) technique. The morphological terminology adopted for *Chaetoceros* in this work follows mainly the proposals of Brunel (1972), Rines & Hargraves (1988), and Bosak & Sarno (2017).

Strain isolation and maintenance

All strains were isolated as monoclonal cultures by single-chain pipetting from material concentrated on a 20 µm mesh, using glass capillaries and an inverted light microscope. The cultures were maintained at the Institut de Ciències del Mar in f/2 + Si medium

Table 1. Information of the different *Chaetoceros* strains isolated in this study, including the GenBank accession numbers of molecular sequences obtained. See Fig. 1 for location of the sampling stations.

Species	Date of isolation	Strain code	Collection site	Coordinates Lat N, Long E	SSU rDNA	LSU rDNA
C. salsugineus[a]	24 May 2016	ICMB61	Barcelona coast (St. 1.4)	41°22.542', 2°12.972'		MW561287
C. salsugineus[a]	24 May 2016	ICMB64	Barcelona coast (St. 1.4)	41°22.542', 2°12.972'	MW561277	MW561288
C. salsugineus[a]	19 Feb 2018	ICMB70	Barcelona coast (St. 1.4)	41°22.542', 2°12.972'	MW561278	MW561289
C. olympicus	13 Mar 2018	ICMB72	Olympic Harbour – Barcelona (St. H)	41°23.074', 2°12.001'	MW561279	MW561290

[a]*C. tenuissimus* after this work, see Discussion.

prepared with filtered (0.2 µm pore size) and autoclaved coastal seawater, with a light:dark cycle of 12:12 h, at 16–20°C and illuminated with fluorescent tubes with a photon irradiance of ~100 µmol photons m^{-2} s^{-1}.

Morphological analysis

Strains were examined (photographed and/or measured) with a Leica DMIRB inverted light microscope (LM) equipped with a Prog Res C10plus JENOPTIK/Jena Laser Optik System digital camera. Different cell dimensions (apical, pervalvar and, when possible, transapical axis) were measured from images using the ProgResCapture Pro v.2.8.8 program. For each strain, at least 30 measurements of the apical and pervalvar axes and as many as possible of the transapical axis (between 3–10, depending on the strain) were obtained. For scanning electron microscopy (SEM), several drops of cultures were collected onto 3 µm polycarbonate filters, then washed with a few drops of bottled water and finally left to dry. Filters were mounted on stubs with colloidal silver, gold coated with a Q150R S sputter coated unit (Quorum Technologies, Ltd) and examined under a HITACHI S-3500N SEM (Hitachi High Technologies Co., Tokyo, Japan) with an accelerating voltage of 5 kV at the Electron and Optical Service of the Institut de Ciències del Mar (ICM-CSIC). For transmission electron microscopy (TEM), culture material was deposited on Formvar-coated copper grids, washed with distilled water, air-dried and observed under a JEM-1010 electron microscope (JEOL USA Inc.) operated at 80 kV. TEM micrographs were taken using a Gatan, Orius SC 1000 A1 (Gatan Inc., Pleasanton, California, USA) digital camera at the Scientific and Technological Centres of the University of Barcelona. Most morphological observations were done within the first month from strain isolation.

Molecular analysis

Fifteen ml of cultured strains were centrifuged at 3000 rpm during 15 min. All supernatant was removed and all genomic DNA from the remaining pellet was placed into a 2 ml Eppendorf tube and stored at −80°C. Previous to DNA extraction, the tubes containing the DNA pellets were subjected to three rounds of freezing/thawing at −80°C until processed. This facilitated the break-up of cell walls. DNA was extracted using the Qiagen Blood & Tissue extraction kit, following the manufacturer's instructions. The resulting purified DNA was used as a template to obtain the complete or partial SSU and partial LSU rDNA sequences. Different approaches (see below) were followed to obtain the sequences for all strains, although for the ICMB61 strain, only the LSU rDNA could be obtained.

The SSU rDNA sequences of ICMB64 strain was obtained using 2 µl of purified DNA as template. The 50 µl PCR reaction contained 1× Buffer, 0.4 µM of primers EukA-EukB (Medlin *et al.*, 1988), 1.5 mM $MgCl_2$, 0.2 mM of each dNTP, and 1 U of Taq DNA polymerase (Invitrogen). For ICMB70 strain, 1 µl of purified DNA was used as template and the 5Prime Hot Master mix (Quantabio) was used for a 25 µl PCR mixture including 1× Master Mix containing 2.5 mM Mg^{2+}, 1 µL BSA, 0.2 mM of each dNTP, 0.5 µM of primers EukA-EukB and 1 U Taq DNA Polymerase. In all cases, PCR conditions were as follows: initial denaturation for 3 min at 94°C, 39 cycles of 45 s at 94°C, 1 min at 55°C, and 3 min at 72°C, followed by a final extension step for 10 min at 72°C.

The partial LSU rDNA sequences (D1–D3 domains) of ICMB61 and ICMB64 were obtained using 1 µl of purified DNA as template. The 50 µl PRC mixture contained 1× Buffer, 1.5 mM $MgCl_2$, 0.2 mM of each dNTP, 0.5 µM of primers D1R (Scholin *et al.*, 1994) and D3B (Nunn *et al.*, 1996), and 1 U of Taq DNA polymerase (Invitrogen). For ICMB70, the 5Prime Hot Master Mix (Quantabio) was used under the same conditions as before and using primers D1R–D3B. The PCR conditions for this primer pair were as follows: initial denaturation for 5 min at 95°C, 39 cycles of 20 s at 95°C, 30 s at 55°C, and 90 s at 72°C, followed by a final extension step of 10 min at 72°C.

Finally, 1 µl of purified DNA of ICMB72 strain was used as a template to amplify the partial SSU rDNA using primers EK-82F and 1520R (DeLong, 1992), and the partial LSU rDNA (D1–D2 domains) using primers D1R and D2C (Scholin *et al.*, 1994). In both cases, the PCR mixture contained 1× Buffer, 1.5 mM $MgCl_2$, 0.2 mM of each dNTP, 0.4 µM of each primer and 2 U of Taq Platinum DNA polymerase (Invitrogen). PCR conditions were as follows: initial denaturation for 5 min at 95°C, 35 cycles of 20 s at 95°C, 30 s at 55°C, and 1 min at 72°C, followed by a final extension step for 7 min at 72°C. In all cases, a 4 µl subsample of the PCR products was electrophoresed for 30 min at 120 V in a 1.2% agarose gel and then visualized under UV illumination. Purification and sequencing were carried out by an external service (Genoscreen, France), using forward, reverse primers (and internal when needed) for all primer pairs and a 3730XL DNA sequencer.

The sequences obtained were aligned with a selection of sequences covering the diversity of *Chaetoceros*, as well as representatives of other diatom genera that served as outgroup, using the online version of MAFFT (Katoh *et al.*, 2019) under the 'auto' option. Subsequently, the alignments were trimmed using trimAl (Capella-Gutiérrez *et al.*, 2009) under the 'gappyout' option. Resulting alignments had 1606 positions for SSU rDNA, and 758 for LSU rDNA. The best-fit model of

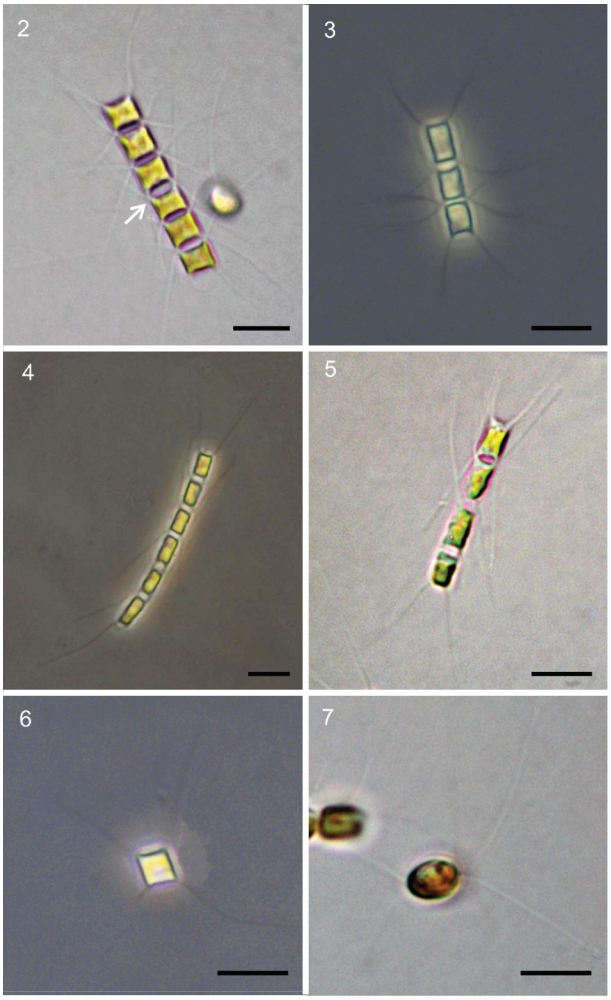

Figs 2–7. *Chaetoceros salsugineus* (*C. tenuissimus* after this work, see Discussion): culture material in LM. **Figs 2, 3, 4, 5**. Complete chain (2) strain ICMB64, arrow shows the separation valve zone of the chain; (3) strain ICMB70, (4) and (5) strain ICMB61; **Fig**. **6**. Solitary cell, strain ICMB64; **Fig**. **7**. Cell in valve view, strain ICMB64. Scale bars: 10 µm.

nucleotide substitutions was evaluated using jModelTest2 (Darriba *et al*., 2012). For the SSU and LSU rDNA alignments, the GTR+G was selected under the Akaike information criterion (AIC) and was then used to infer maximum likelihood (ML) and Bayesian phylogenetic trees. Maximum-likelihood phylogenetic analyses were performed with RAxML 8.0.0 (Stamatakis, 2014), using a GTRGAMMA model and 1000 runs with distinct random starting trees. Bootstrap analysis was done with 1000 pseudoreplicates. Bayesian inference was run with MrBayes 3.2 (Ronquist *et al*., 2012), using a GTR model and four Markov chains with one million cycles for each chain. Bayesian posterior probabilities were obtained from the post-burn-in consensus tree. All sequences obtained were deposited in GenBank (Table 1).

Results

Morphological studies

Based on morphological observations, the strains ICMB61, ICMB64 and ICMB70 were identified as *C. salsugineus*, while strain ICMB72 resulted in a new species: *C. olympicus* sp. nov. The morphological characteristics of both species are described below.

C. salsugineus Takano (1983). Figs 2–16

Cells solitary or united into delicate short to medium (up to 12 cells) size chains, normally straight but sometimes slightly bent (Figs 2–5). The cells are square or rectangular in girdle view and elliptical in valve view (Figs 2–7). Cell size: 2.9–6.0 µm in the apical axis, 3.9–10.3 µm in the pervalvar axis, and 3.0–4.8 µm in the transapical axis (Table 2). One large chloroplast per cell is present. The terminal setae lie in the apical plane and usually emerge at an angle of almost 45° from the chain axis. In some cells, terminal setae open outwards at their distal part (bell shaped) (Figs 2–6) and in a few cases, they run parallel to the chain axis. The intercalary setae generally emerge from the chain axis at the same angle as the terminal ones (45°), although in some intercalary setae this angle is more closed (almost 30°; Fig. 2); in the distal part, they are generally oriented almost perpendicularly to the chain axis (Figs 2, 3). In strain ICMB61, all the terminal and intercalary setae were oriented at an angle of 30° and some ran distally almost parallel to the chain axis (Figs 4, 5). Sibling setae diverge with respect to the apical axis at an angle of about 40° (Brunel Group II; Fig. 7). Setae arise at the corner of the cells and sibling setae cross at the chain edge, without basal part (Figs 8–11). The aperture is narrowly lanceolate to elliptical (Figs 2–5). There is a slit-shaped rimoportula with external tube in the terminal valves and every 2–3 sibling cells coinciding with closed angles in setae (Fig. 8). In strain ICMB61, the rimoportula was found in the terminal and in all the observed cells from a chain (Fig. 9). The mantle is short and the valve face flat or concave (Figs 10–15). A high or low hyaline rim (Figs 11, 12, respectively) is present along the marginal ridge that separates the valve face from the mantle. In poorly silicified cells, the different bands that compose the girdle may be observed (Fig. 13). Valve with radial pattern of costae, which branch towards the edge (Fig. 15). Setae are thin and circular in cross-section with strongly twisted rows of small rectangular poroids (26.9 ± 1.7 poroids in 1 µm, n = 7) and several spines arranged in spiral (Fig. 16). Resting spores were not observed.

***Chaetoceros olympicus* Arin & Reñé sp. nov.**
Figs 17–43

DIAGNOSIS: Poorly silicified solitary or chain-forming organisms. Cells are square or rectangular in girdle view and elliptical in valve view. One chloroplast per cell. Cell size: 3.4–10.5 µm in the apical axis, 4.0–11.6 µm in the pervalvar axis, and 3.8–5.0 µm in the transapical axis. Aperture narrowly lanceolate. Terminal setae emerge at an angle of almost 45° from chain axis while intercalary ones are generally perpendicular or slightly inclined towards one end of the chain. Setae diverge equally from the apical axis at an angle of about 30°. Absence of rimoportula in intercalary and terminal valves; valve face flat. Setae are thin and circular in cross-section with few slightly twisted rows of small rectangular poroids. Resting spores with primary valve vaulted and covered with short to medium-sized spines and secondary valve smaller, rounded and smooth.
HOLOTYPE: Designated here as SEM stub deposited in the Biological Collections (CBR) at the Institut de Ciències del Mar (ICM-CSIC, Barcelona, Spain) under the catalogue/accession number ICMCBR0 00463 (Guerrero *et al.*, 2020). Molecular characterization (GenBank accession numbers): SSU rDNA: MW561279; LSU rDNA: MW561290.
TYPE LOCALITY: Port Olímpic (Eng.: Olympic Harbour) (41°23.07′N, 2°12.0′E), Barcelona, Spain.
HABITAT: Marine.
ETYMOLOGY: Named for the location where the species was isolated (Port Olímpic).
Observations: Poorly silicified solitary cells or united into delicate short to medium-sized chains, usually slightly bent. Cells are square or rectangular in girdle view and elliptical in valve view (Figs 17–20 and 22–24). One large chloroplast per cell is present. Terminal setae usually arise straight at the corner of the cell at an angle of 45° from the chain axis (Figs 17, 18, 23, 24). The intercalary setae emerge from the corners of the cells, cross at the chain edge, without basal part (Figs 25, 29), and run perpendicular to the chain axis or slightly oriented towards one end of the cell (Figs 17, 18, 23), although some intercalary setae of a chain can emerge at an angle of around 45° (Figs 17, 23). Sibling setae diverge equally from the apical plane at an angle of about 30° (Brunel Group II; Fig. 19). The aperture is narrowly lanceolate (Figs 17, 18, 23). Absence of rimoportula in intercalary and terminal valves (Figs 25–29). Valve mantle low (Figs 27, 29). Valve face flat (Figs 28, 29). Setae are thin and circular in cross-section with few slightly twisted rows of small rectangular poroids (16.7 ± 1.1 poroids in 1 µm, n = 9) and some spines arranged in spiral (Figs 30, 31). Resting spores closer to one of the valves (Figs 20, 22). Primary valve of the resting spore vaulted and covered with short to medium-size d spines, secondary valve rounded, smaller than primary valve and smooth (Figs 20–22 and 32).

Two morphometrically different morphotypes of this species are observed, each related to a different stage of its life cycle (see below): (1) morphotype 1 (Figs 17–22): Isolated from natural marine sample. Apical axis: 3.4–5.2 µm, pervalvar axis: 6.1–11.6 µm, transapical axis: 3.8–5.0 µm; (2) morphotype 2 (Figs 23, 24): Observed in culture. Apical axis: 8.0–10.5 µm, pervalvar axis: 4.0–9.8 µm (Table 2).
LIFE CYCLE: Strain ICMB72 was originally isolated from a morphotype 1 chain (Fig 33). After 22 days of cultivation, an auxospore-like formation was observed only in terminal cells of a number of chains (Figs 34–37). Likewise, the presence of solitary cells and short chains with a different morphometry (morphotype 2, Figs 40, 41) was observed, although with predominance of morphotype 1. The life cycle of this species could be established as follows. A terminal cell expands forming an auxospore-like structure (Figs 34–36). A new enlarged cell is formed within the expanded auxospore-like structure (Fig. 37) which detaches from the chain (Fig. 38). A funnel-shaped empty terminal frustule remains on the original chain (Fig. 39). A new chain with the characteristics of morphotype 2 (Fig. 40) was formed from the initial cell. The new chains divided mitotically forming longer chains (Fig. 41). The presence of gametes has not been observed. On the other hand, in field samples, the formation of resting spores and a higher percentage of solitary cells was observed (Figs 42, 43) in morphotype 1 after two weeks of the maximum abundance of chain-forming cells (Table 3). In culture, and less frequently, solitary cells (Fig. 24) and resting spore formation was also observed in morphotype 2.

Table 2. Morphometric data of the different *Chaetoceros* strains, including measurements of the apical and pervalvar axis (n = 30–34 cells) and transapical axis (n = 3–10 cells). The values indicate mean ± SD, with minimum and maximum values in parentheses.

Species	Apical axis (µm)	Pervalvar axis (µm)	Transapical axis (µm)
C. salsugineus[a] (ICMB61)	3.3 ± 0.3 (2.9–4.0)	6.1 ± 1.1 (4.6–10.3)	3.7 ± 0.2 (3.6–4.0)
C. salsugineus[a] (ICMB64)	5.3 ± 0.3 (5.8–6.0)	4.9 ± 0.8 (3.9–7.2)	4.5 ± 0.3 (4.6–4.8)
C. salsugineus[a] (ICMB70)	3.7 ± 0.2 (3.2–4.1)	6.7 ± 1.2 (4.7–9.9)	3.6 ± 0.3 (3.0–4.1)
C. olympicus (ICMB72) Morph1	4.1 ± 0.4 (3.4–5.2)	8.5 ± 1.3 (6.1–11.6)	4.5 ± 0.5 (3.8–5.0)
C. olympicus (ICMB72) Morph2	9.1 ± 0.7 (8.0–10.5)	5.9 ± 1.7 (4.0–9.8)	

[a]*C. tenuissimus* after this work, see Discussion.

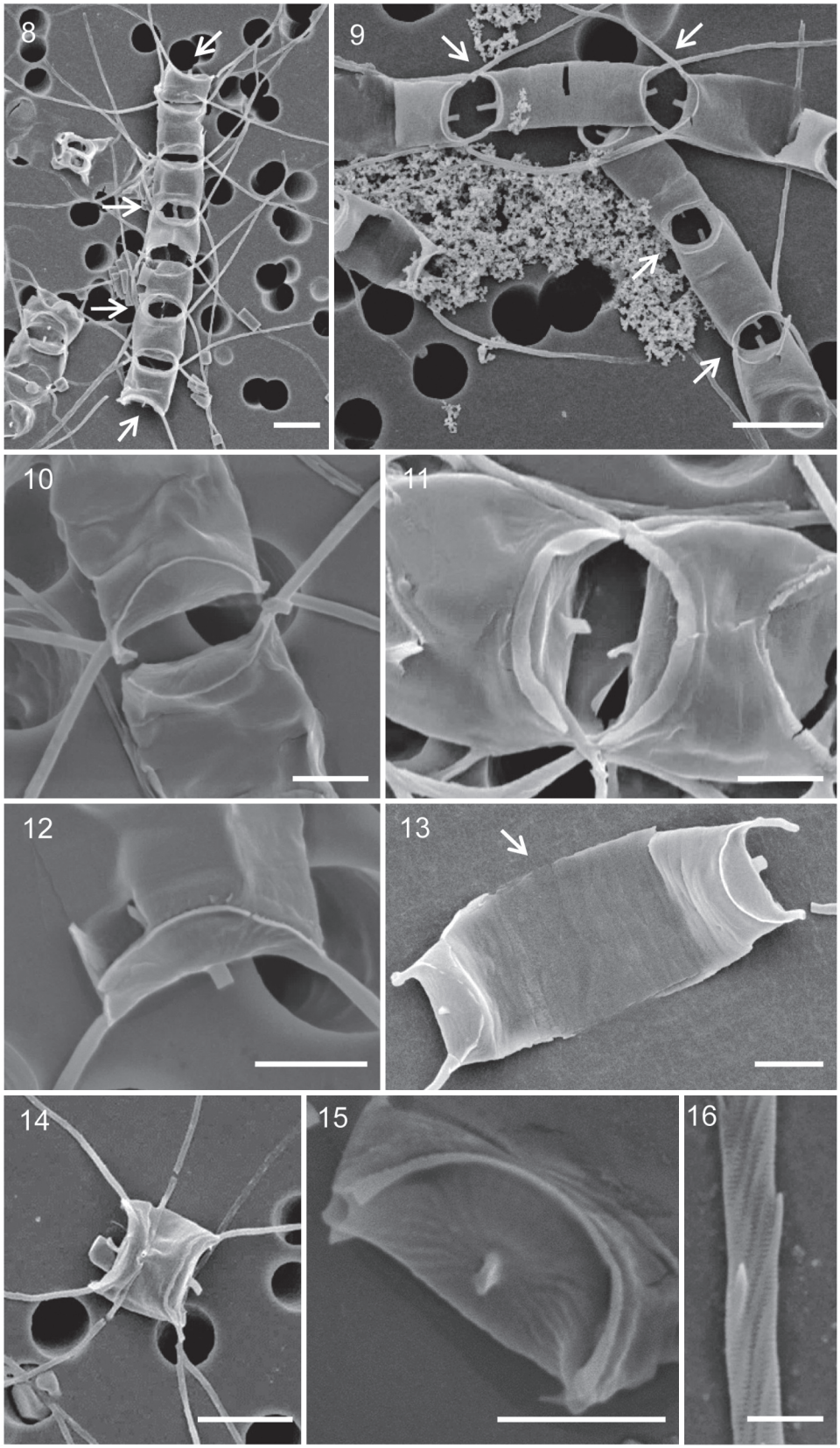

Figs 8–16. *Chaetoceros salsugineus* (*C. tenuissimus* after this work, see Discussion): culture material in SEM. **Fig**. **8**. Complete chain showing the presence of rimoportula (arrows) in terminal and in some sibling valves, strain ICMB64. **Fig**. **9**. Complete chain showing the presence of rimoportula (arrows) in terminal and all sibling cells, strain ICMB61. **Fig**. **10**. Sibling intercalary valves without rimoportula, strain ICMB70. **Fig**. **11**. Sibling cells with a rimoportula in their valves, strain ICMB64. **Fig**. **12**. Detail of a terminal cell, strain ICMB70. **Fig**. **13**. Weakly silicified cell showing the different bands of the girdle (arrow), strain ICMB61. **Fig**. **14**. Solitary cell, strain ICMB64. **Fig**. **15**. Detail of a terminal valve, strain ICMB70. **Fig**. **16**. Detail of setae, strain ICMB64. Scale bars: Figs 8, 9, 14, 5 µm; Figs 10–13, 15, 2 µm; Fig. 16, 0.5 µm.

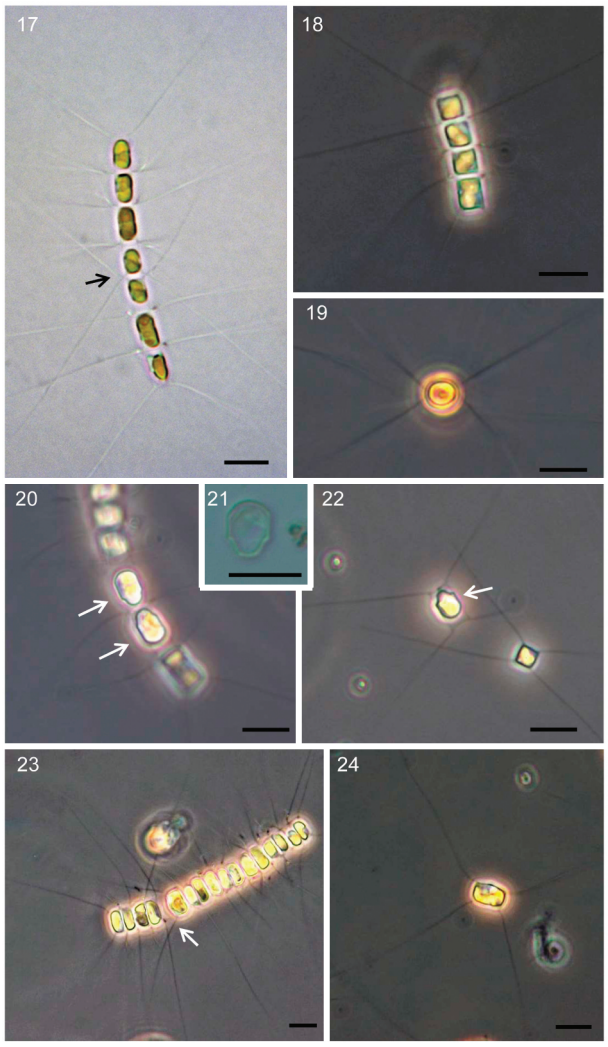

Figs 17–24. *Chaetoceros olympicus*: Field and culture material in LM. **Fig. 17**. Complete chain of morphotype 1, arrow shows the separation valves zone of the chain, culture. **Fig. 18**. Complete chains of morphotype 1, field. **Fig. 19**. Cell in valve view, culture. **Fig. 20**. Complete chains of morphotype 1, arrows show resting spores, field. **Fig. 21**. Detail of a resting spore, field. **Fig. 22**. Solitary cells of morphotype 1, one with a resting spore (arrow), field. **Fig. 23**. Complete chain of morphotype 2. Arrow shows the separation valves zone of the chain, culture. **Fig. 24**. Solitary cell of morphotype 2, culture. Scale bars: 10 µm.

Phylogenetic analyses

The SSU rDNA sequences obtained for strains ICMB64, 1753 base pairs (bp) long, and ICMB70 (1771 bp) were identical. They were also identical to several sequences from GenBank attributed to *C. tenuissimus* (strains Na14C1, SZN-B430, newCA3, newGB2a, Na44A1, Na26A1), but also to others identified as *C. dayaensis* (strains MC107L, MC107S) or as *Chaetoceros* sp. (strain RCC5795). The phylogenetic tree (Fig. 44) showed the sequences obtained in this study and those belonging to *C. tenuissimus* clustered together with maximum support and forming a sister branch (100%/1) with sequences belonging to *Chaetoceros neogracilis*. Another clade was obtained (98%/1), grouping sequences belonging to *C. coloradensis, C. muellerii* and further sequences identified as *C. neogracilis*. Altogether, they formed the *Simplicia* section (according to De Luca *et al.*, 2019*a*), even though the statistical support was low (–/0.9). The closest species to *Simplicia* representatives were grouped in a cluster (95%/1) encompassing the *Socialis* section (100%/1), including *C. socialis, C. debilis* and *C. sporotruncatus* among others, the *Furcellata* section (100%/1) including *C. radicans* and *C. cinctus*, and the *Costata* section, including *C. costatus*.

The SSU rDNA sequence obtained for ICMB72 was 1613 bp and identical to sequences identified as *C.* cf. *wighamii* (strains RCC3008 and DM53) and an environmental sequence (FR874617), and 99.9% similar to *C.* cf. *wighamii* strain BH65. It formed a cluster with maximum support with those sequences and also with a second environmental sequence and a further sequence identified as *C.* cf. *wighamii* (strain BH46). Those sequences were grouped in a cluster (even though under low statistical support, –/0.95), with *Minima* section representatives, i.e. *C. throndsenii*, and *Dicladia* representatives, including *C. elegans, C. mannaii, C. lorenzianus* and *C. mitra*. An additional sequence from GenBank identified as *C. wighamii* RCC3007 was detected, but it was identical to sequences belonging to *C. gelidus* and included within the *Socialis* section, probably representing a misidentification.

The LSU rDNA sequences obtained for strains ICMB61, ICMB64 and ICMB70 (868, 867 and 816 bp long, respectively) showed 3 mismatches (2 of them corresponding to ambiguities) among them. Those sequences agreed with all *C. tenuissimus* sequences available from GenBank, with similarities ranging from 99.6–99.8% and clustered together with maximum support (Fig. 45). *Chaetoceros tenuissimus* sequences formed a sister taxon (100%/1) with sequences of *C. neogracilis*, and a sequence identified as *Chaetoceros* sp. CCMP163. The *Simplicia* section was also obtained (97%/1), including a cluster comprising C. *gracilis, C. muellerii* and *C. coloradensis* (100%/1). As previously observed, the *Simplicia* section formed a sister cluster (100%/1) with sections *Socialia, Furcellata* and *Costata*.

The LSU rDNA sequence obtained for ICMB72 (537 bp) was identical to a sequence labelled as *C.* cf. *wighamii* RCC3008 (strain isolated from the Baltic Sea). They did not show a close phylogenetic relationship with any other sequence, but clustered in a clade (70%/0.98) including *Dicladia* (73%/0.94), and *Minima* (95%/1) sections. Another sequence identified as *C. wighamii* SAL1 was available. It clustered independently to the previous sequences and did not show a close phylogenetic relationship with any other sequence available. Finally, a sequence labelled as *C. wighamii* RCC3007 was also available, but in this case, it was identical to sequences corresponding to *C. gelidus*.

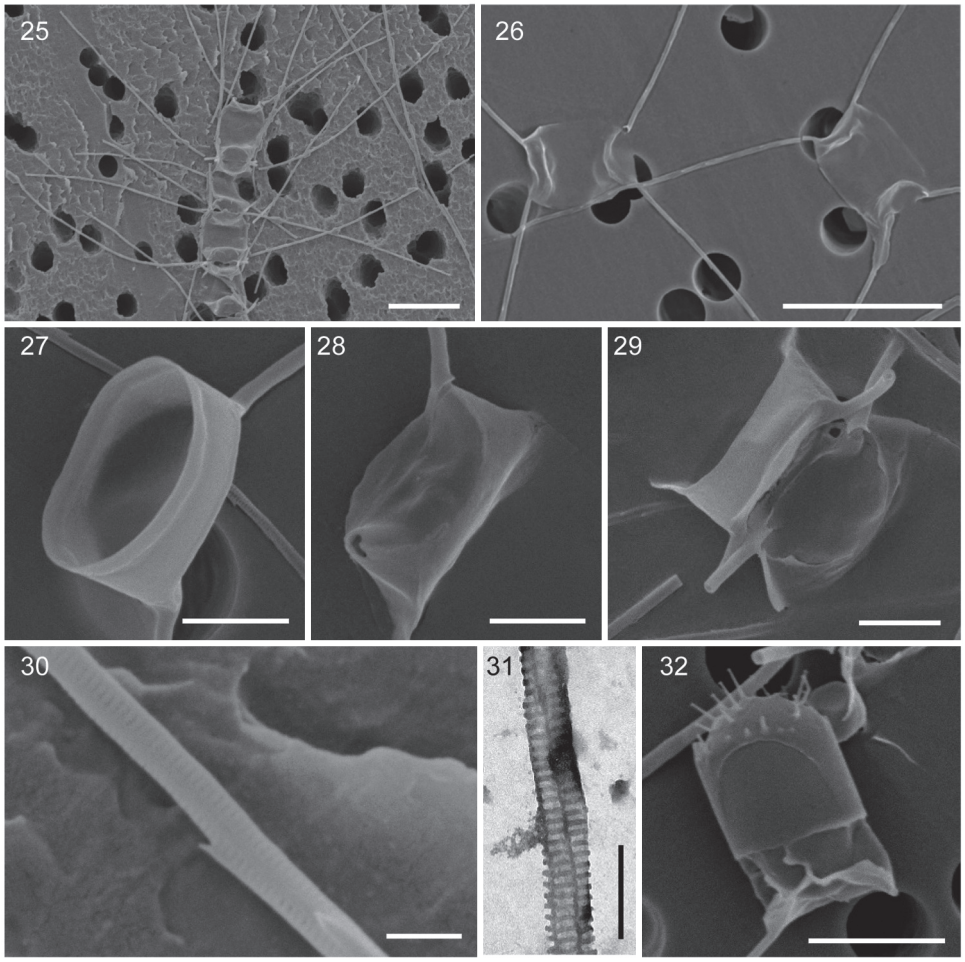

Figs 25–32. *Chaetoceros olympicus*: Field and culture material in SEM and TEM. **Fig. 25**. Part of a chain of morphotype 1, field. **Fig. 26**. Solitary cells of morphotype 1, field. **Fig. 27**. Internal view of valve and mantle of a morphotype 1 cell, culture. **Fig. 28**. Terminal cell (morphotype 1) showing the absence of rimoportula in the valve, culture. **Fig. 29**. Intercalary cells (morphotype 1) showing the fusion point of the setae, culture. **Figs 30, 31**. Detail of a seta in SEM and TEM views, respectively, field and culture. **Fig. 32**. Resting spore with the secondary valve still surrounded by the theca of the vegetative cell, field. Scale bars: Figs 25, 26, 10 µm; Figs 27–29, 2 µm; Figs 30, 31, 0.5 µm; Fig. 32, 5 µm.

Ecology

Chaetoceros salsugineus

Chain-forming cells of *C. salsugineus* presented maximum abundances in spring, with values exceeding 10^5 cells l^{-1} in 2017. The chains decreased in abundance in late spring and were not detected during the summer (Table 3) and autumn months (data not shown). In winter, low abundances of *C. salsugineus* chains were found (< 1.3×10^3 cells l^{-1}). Solitary cells of this species were only observed in 2017 in the months following the disappearance of chain-forming forms, with a maximum abundance in early summer of around 1.6×10^4 cells l^{-1}. They were not detected in autumn (data not shown), winter and spring (Table 3).

The chain-forming organisms were observed within a temperature range between 12.8 and 19°C, while solitary cells were found between 22.2 and 26.4°C. Chain and solitary forms were found at a salinity range between 37.8 and 38.3. Inorganic nutrient concentrations were comparable when chain and solitary forms reached their respective maxima, with only slightly higher concentration of ammonium and nitrate at the maximum of the solitary form (Table 3).

Chaetoceros olympicus

In the first sampling carried out in the Olympic harbour, *C. olympicus* (morphotype 1) was detected at relatively high abundance (around 5.3×10^5 cells l^{-1}). The dynamics of this morphotype was followed until it disappeared. At that moment, the correspondence of morphotype 2 to *C. olympicus* had not been established and its presence could have been overlooked. Morphotype 1 appeared at temperatures between 13.2 and 17.6°C, and salinities between 36.2 and 38.2 and, in general, with relatively high concentrations of inorganic nutrients, except for phosphate (Table 3). The maximum abundance of this morphotype (chain and solitary forms) was observed in the second half of March, although its presence was observed until the beginning of May (Table 3).

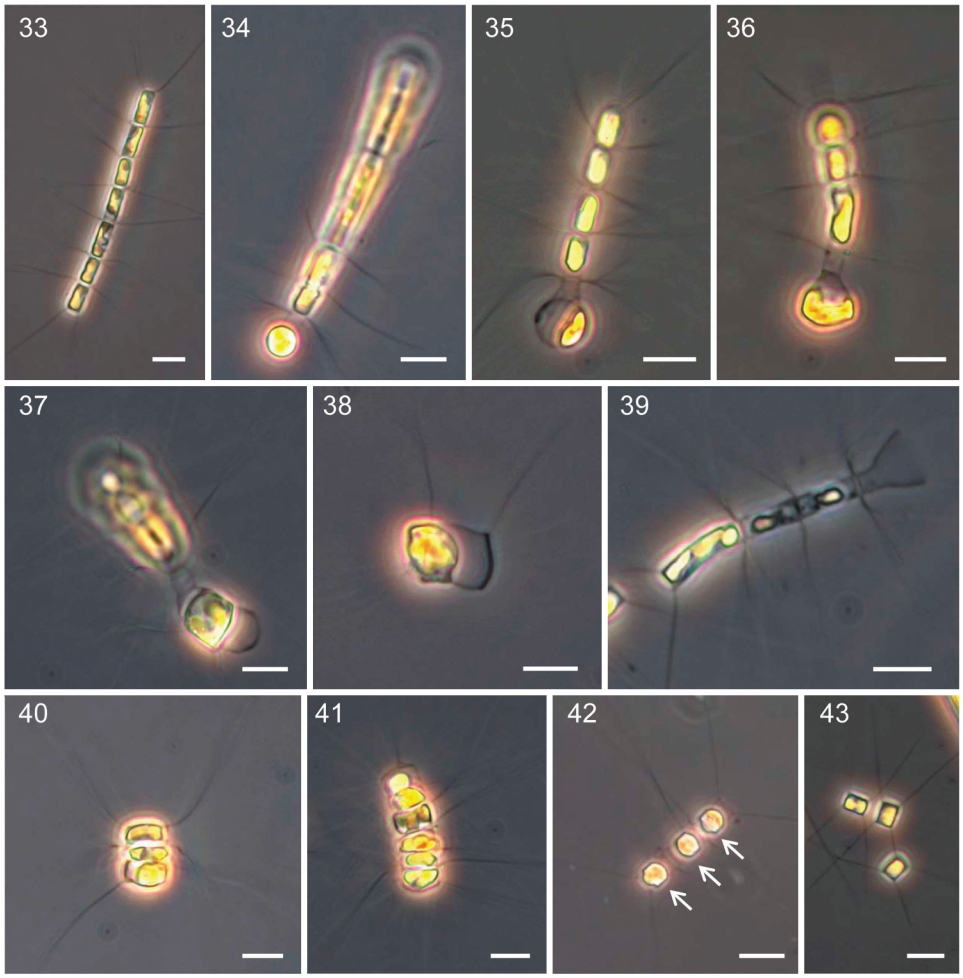

Figs 33–43. Life cycle of *Chaetoceros olympicus*, LM. **Fig. 33**. Complete chain of morphotype 1, culture. **Figs 34–37**. Process of forming an auxospore-like structure in a terminal cell of morphotype 1 chains, culture. **Fig. 38**. Initial cell, culture. **Fig. 39**. Chain (morphotype 1) with a funnel-shaped empty terminal frustule, culture. **Figs 40**, **41**. New complete chain of morphotype 2, culture. **Figs** 42, **43**. Chain-forming and solitary cells of morphotype 1, some of them with resting spores (arrows), field. Scale bars: 10 µm.

Discussion

A re-examination of morphological and molecular information available from this study and from the literature provided evidence that *C. tenuissimus* and *C. salsugineus* were the same species. *Chaetoceros tenuissimus* (Meunier, 1913) was originally described as solitary organisms and its ability to form colonies was only recently recognized (Gaonkar *et al.*, 2018). This probably explains why Takano (1983) described the chain-forming specimens from the Sea of Japan as the new species *C. salsugineus*, although a solitary form was recognized in his description. However, subsequent observations of *C. salsugineus* highlighted the morphological and ultrastructural similarity of this species with *C. tenuissimus* (Trigueros *et al.*, 2002; Bosak, 2013).

A number of strains morphologically identified as *C. salsugineus* in this study shared identical LSU rDNA sequences with morphologically described *C. tenuissimus* strains from the Gulf of Naples (Kooistra *et al.*, 2010; Gaonkar *et al.*, 2018; De Luca *et al.*, 2019*a*). Both taxa share the same pattern of valve ornamentation, morphology of the setae and the rimoportula, and the presence of a hyaline rim along the marginal ridge. Because the original description of *C. salsugineus* (Takano, 1983) also included ultrastructure details of the species (based on TEM observations) we were able to correctly identify our material. There is another LSU rDNA sequence in GenBank (KP175041) corresponding to strain CPH16 and identified as *C. salsugineus* (Li *et al.*, 2015) based only on LM observations (Li, Y. pers. comm.). However, later, the same sequence was assigned to *C. neogracilis* based on thoroughly described material from the Beaufort Sea (Balzano *et al.*, 2017). Even though the morphology of *C. salsugineus* and *C. neogracilis* is very similar under light microscopy, the valve ornamentation of the two species is different (see Takano, 1983: fig. 14; Balzano *et al.*, 2017: fig. 8J, K). Thus, the taxonomic assignment of the strain CPH16 to *C. salsugineus* is probably wrong (Li, Y. pers. comm.). Although the molecular information of *C. tenuissimus* and *C. salsugineus* was not obtained

Table 3. Physicochemical variables (temperature, salinity and inorganic nutrients), chlorophyll-*a* (Chl-*a*) and *Chaetoceros* abundance for (a) Surface waters at the Barcelona coast (St 1.4) and (b) surface waters at the Olympic Harbour (St. H).

a)

Date	Temp. (°C)	Salinity	Phosphate (µM)	Ammonium (µM)	Nitrite (µM)	Nitrate (µM)	Silicate (µM)	Chl-*a* (µg l^{-1})	*C. salsugineus*[a] chain-forming (cells l^{-1})	*C. salsugineus*[a] solitary (cells l^{-1})
16/02/2017	13.4	38.2	0.15	3.59	0.25	2.33	2.02	1.14	1284	0
22/03/2017	14.2	38.0	0.03	0.62	0.12	1.64	1.91	0.71	0	0
25/04/2017	15.8	38.1	0.04	0.10	0.08	0.10	0.78	0.86	130335	0
23/05/2017	18.2	38.2	0.06	0.10	0.08	0.24	0.23	0.66	337	0
22/06/2017	22.2	38.0	0.03	0.43	0.10	0.20	0.80	0.30	0	15916
17/07/2017	25.9	38.0	0.02	0.62	0.06	0.09	0.72	0.06	0	692
10/08/2017	26.4	38.1	0.04	0.54	0.10	0.10	0.87	0.35	0	692
23/01/2018	13.4	38.3	0.25	4.27	0.52	4.92	2.34	1.03	255	0
19/02/2018	12.8	38.1	0.10	4.89	0.66	3.24	1.69	0.90	45	0
14/03/2018	13.1	38.3	0.07	0.73	0.36	2.70	1.22	3.35	533	0
26/04/2018	17.7	37.0	0.12	10.39	0.79	4.47	1.64	0.67	0	0
30/05/2018	19.0	37.8	0.03	1.04	0.05	0.14	0.80	0.22	65	0

b)

Date	Temp. (°C)	Salinity	Phosphate (µM)	Ammonium (µM)	Nitrite (µM)	Nitrate (µM)	Silicate (µM)	Chl-*a* (µg l^{-1})	*C. olympicus*[b] chain-forming (cells l^{-1})	*C. olympicus*[b] solitary (cells l^{-1})
13/03/2018	13.2	37.5	0.09	3.85	0.29	1.56	3.91	1.64	524582	2916
27/03/2018	13.4	37.9	0.06	1.16	0.13	0.39	1.15	1.68	2050	51013
05/04/2018	14.0	38.2	0.07	5.50	0.22	1.19	1.10	0.89	129	47
17/04/2018	14.6	36.2	0.39	5.73	0.51	12.18	8.09	0.92	600	0
25/04/2018	17.6	36.7	0.05	3.79	0.64	9.25	3.71	0.67	0	0
04/05/2018	15.2	37.1	0.14	2.42	0.25	2.69	1.64	0.71	0	13

[a]*C. tenuissimus* after this work, see Discussion;[b]morphotype 1.

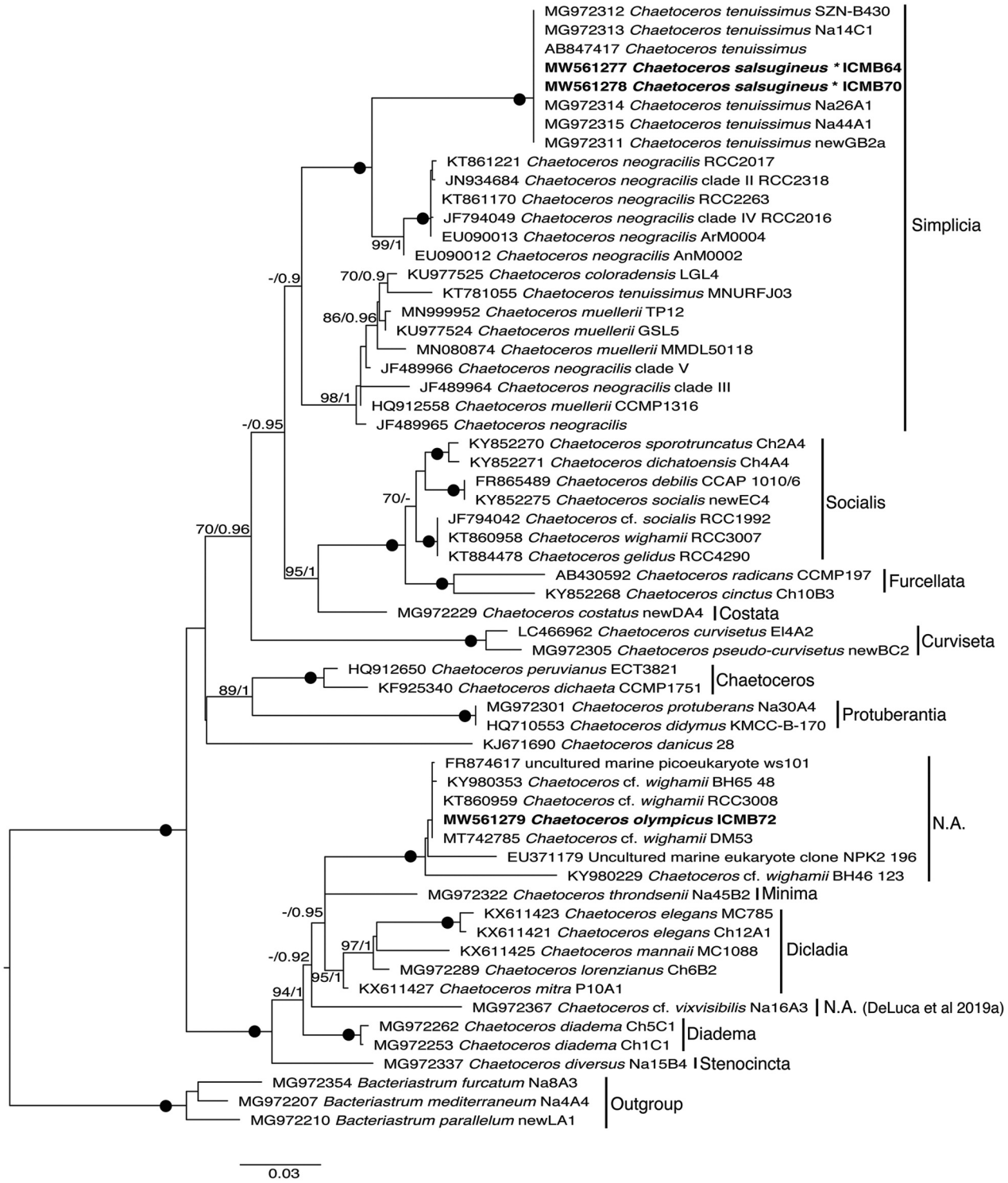

Fig. 44. SSU rDNA phylogenetic tree including sequences of some *Chaetoceros* representatives of interest and sequences obtained in this study (in bold). Sequences of *Ditylum brightwellii, Attheya* sp. and *Hemiaulus hauckii* were used as outgroup. Statistical support shown in nodes corresponds to boostrap values (%) and Bayesian posterior probability. Only values >70% and 0.95 respectively are shown and black dots represent maximum statistical support. The different phylogenetic clusters were labelled according to morphological sections proposed in De Luca *et al.* (2019*a*). N.A. = species not assigned to any existing section. **C. tenuissimus* after this work, see Discussion.

from the type locality material (North Sea and Sea of Japan, respectively), the molecular sequence shared by both taxa was detected in environmental sequencing in their respective type localities and also in other areas of the world (see De Luca *et al.*, 2019*b* as *C. tenuissimus*). This suggests correct taxonomic assignment of these sequences and supports that the description of ultrastructural details of *C. tenuissimus* made on material from a non-type locality zone, corresponds to the species described by Meunier (1913). Following the original description (Takano, 1983), *C. salsugineus* was frequently

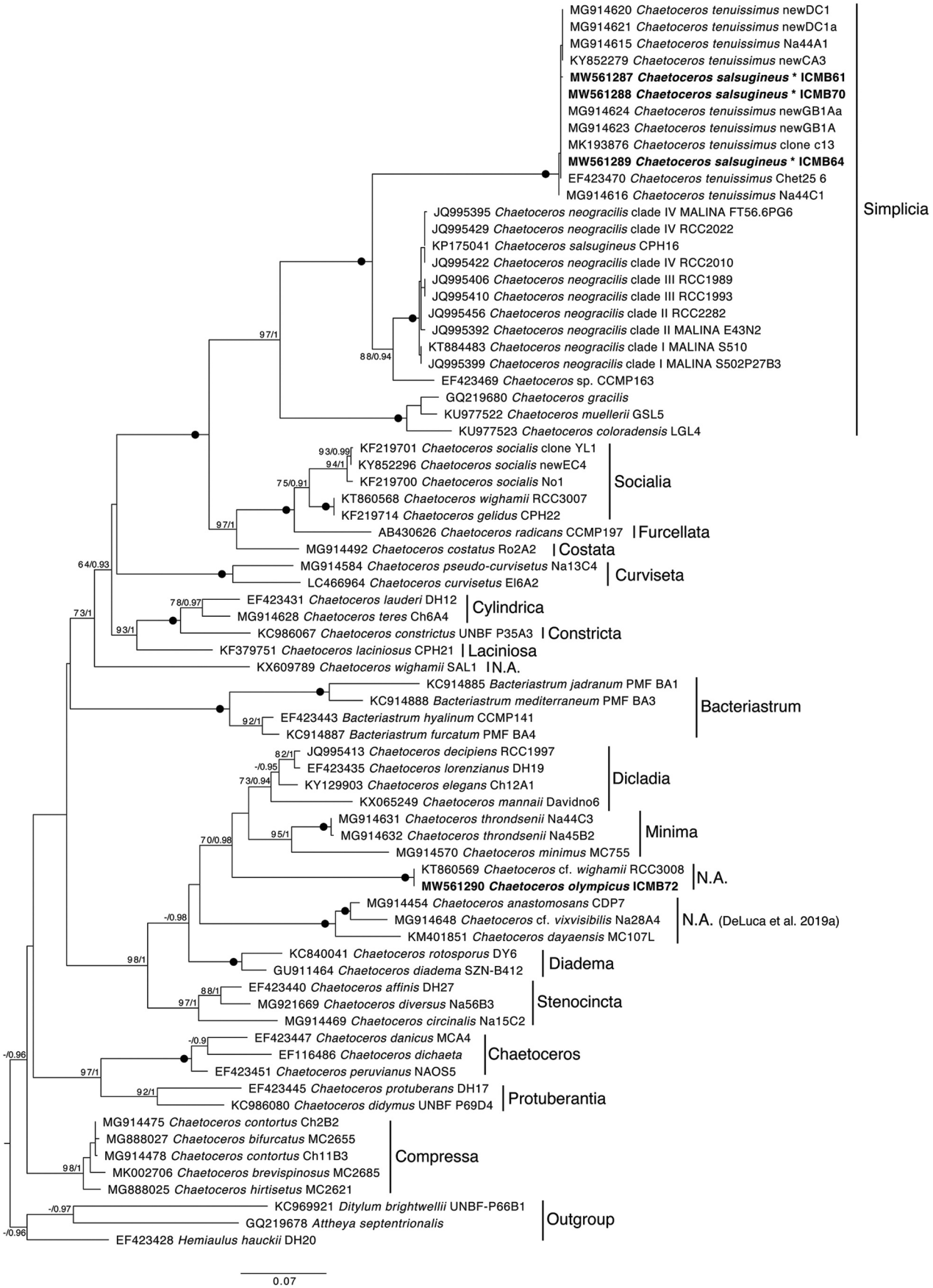

Fig. 45. LSU rDNA phylogenetic tree including sequences of some *Chaetoceros* representatives of interest and sequences obtained in this study (in bold). Sequences of *Bacteriastrum* species were used as outgroup. Statistical support shown in nodes corresponds to boostrap values (%) and Bayesian posterior probability. Only values >70% and 0.95 respectively are shown and black dots represent maximum statistical support. The different phylogenetic clusters were labelled according to morphological sections proposed in De Luca *et al.* (2019*a*). N.A. = species not assigned to any existing section. **C. tenuissimus* after this work, see Discussion.

reported from other coastal (bays and estuaries) Japanese waters, where, in some cases, the solitary form reached bloom abundances (Orlova & Selina, 1993; Orlova & Aizdaicher, 2000; Shevchenko *et al.*, 2006; Ichimi *et al.*, 2012). On the other hand, *C. tenuissimus* was also reported at high abundances in Japanese coastal waters (Tomaru *et al.*, 2018) and its V4-SSU rDNA sequence was found in an environmental sample from Japan (Lat: 34.32, Long: 135.12; see De Luca *et al.*, 2019*b*). The detection of both taxa in this area, coupled with the molecular and morphological evidence here provided, strongly support our hypothesis that *C. tenuissimus* and *C. salsugineus* are the same species.

Based on these observations, we propose the two species names as synonyms, prevailing *C. tenuissimus* as it is the earliest available name applied to the taxon (therefore and hereafter referred as *C. tenuissimus*). The original description of *C. tenuissimus* (Meunier, 1913) only included one figure with a drawing of the species in apical and valvar view that is formally acceptable as the holotype (Art. 9.4 of ICN). Since this illustration is ambiguous and not interpretable, here we propose an emended diagnosis of the species and designate an epitype with material from coastal waters of Barcelona. The epitype represents the current concept of this species and encompasses all the data needed for modern taxonomic research, including ultrastructural information, recognition of different life forms and molecular signature.

C. tenuissimus Meunier 1913 emend. Arin, Reñé & Sarno

SYNONYM: *Chaetoceros salsugineus* Takano (1983).
HOLOTYPE: *C. tenuissimus* (Meunier): Plate VII, fig. 55 in Meunier (1913).
TYPE LOCALITY: La Mer Flamande – North Sea.
ICONOTYPE: *C. salsugineus* (Takano): figs 2, 3, 5, 6 and 12 in Takano (1983).
TYPE LOCALITY: Osaka Bay (Figs 2, 3 and 6) and Atsumi Bay (Figs 5 and 12), Japanese waters.
EPITYPE: Designated here as SEM stubs deposited in the Biological Collections (CBR) at the Institut de Ciències del Mar (ICM-CSIC, Barcelona, Spain) under the catalogue/accession number ICMCBR000479 (Guerrero *et al.*, 2020).
Molecular characterization (GenBank accession numbers): SSU rDNA: MW561277, MW561278; LSU rDNA: MW561287, MW561288, MW561289.
EPITYPE LOCALITY: Barcelona coast (Station 1.4: 41°22.54′, 2°12.97′), Barcelona, Spain.
Emended diagnosis: Solitary or chain-forming cells. Cells square or rectangular in girdle view and elliptical in valve view. One chloroplast per cell. Aperture narrowly lanceolate to elliptical, sometimes indistinct. Terminal setae oriented parallel to chain axis or diverging at an angle of almost 45°. Intercalary setae diverge at an angle of about 45° from the chain axis and run almost perpendicular in the distal part. Presence of slit-shaped rimoportula in the central area of the terminal valves. Setae thin and circular in cross-section with strongly twisted rows of small rectangular poroids and several spines arranged in spiral. Resting spores not observed.

Description

An unusual characteristic of *C. tenuissimus* is the presence of a rimoportula not only in terminal cells of the chains (as generally typical in *Hyalochaete*) but also in every 2–3 sibling cells, coinciding with a different orientation of their corresponding setae (Takano, 1983; Trigueros *et al.*, 2002; Fig. 8). These features correspond to separation valves, where the chain is going to break into smaller chains. In the strain ICMB61, a rimoportula was found in all valves (Fig. 9), indicating that the observed chains are prepared to pass directly to solitary cells, without going through chains of smaller size.

The cell size and shape of the three strains of *C. tenuissimus* presented differences. In strain ICMB64, cells are square, while strains ICMB61 and ICMB70 cells are rectangular. The mean size of the apical axis of strain ICMB64 is higher than that of strain ICMB61 and strain ICMB70, while the pervalvar axis for the latest strains is longer than that for the ICMB64 strain (Table 2). The varied morphometry of the strains could correspond to different stages of the life cycle or to different growth forms. The elongation of the cells in parallel with apical axis reduction has also been observed in *Chaetoceros dichaeta* (Assmy *et al.*, 2008) over a one-year period. This corresponds to the general scheme of diatom life cycle in which there is a reduction of cell size by successive mitotic divisions, until cells reach a minimum size. When cells exceed a critical size threshold, there is a sexual period (production of female and male gametes) with the formation of auxospores, which result in a new enlarged initial cell (Mann, 2011). Changes in the size and shape of the cells, as well as different life-form prevalence during the growth development of morphotypes classified as *C. salsugineus* were also observed by Orlova & Selina (1993) and Orlova & Aizdaicher (2000) in natural environment and in culture, respectively. During 11 days of culture, Orlova & Aizdaicher (2000) found that actively growing square solitary cells dominated the exponential phase; then the percentage of chains (with 2, 3 or more cells) increased until the stationary phase (during which they observed enlarged cells), and in the end they found cells of different shapes and sizes, although dominated by elongated solitary cells. During a *C. tenuissimus* (as *C. salsugineus*)

bloom in the Sea of Japan, Orlova & Selina (1993) observed mainly chain forms at the beginning, while at the end, with unfavourable environmental conditions, they found a dominance of solitary cells. This agrees with the natural dynamics of these organisms as observed in the Barcelona coast in 2017. We found chains of *C. tenuissimus* from February to May and later (until August) only solitary cells (Table 3).

Chaetoceros tenuissimus is a cosmopolitan species (De Luca *et al.*, 2019*b*) that can produce blooms of up to 10^7 cells l^{-1}. On the coast of Barcelona, chain-forming *C. tenuissimus* reached their maximum abundance in spring (10^5 cells l^{-1}) with a temperature around 16°C and a salinity of 38.1. On the other hand, the solitary form was only found in summer (temperature >20°C, salinity around 38) with a maximum abundance of 10^4 cells l^{-1} (Table 3). This agrees with the long-term observations at LTER-MC station in the Bay of Naples (Mediterranean Sea), where the solitary form was one of the dominant diatom species (up to 10^7 cells l^{-1}) in the summer phytoplankton assemblage (Ribera D'Alcalà *et al.*, 2004). At LTER-MC station, the colonial form of the species, previously named as *C.* cf. *wighamii*, was reported at low concentration in late spring (Sarno, D. unpublished data). Rines & Hargraves (1988) also found high abundances (10^7 cells l^{-1}) of the solitary form in Narragansett Bay (USA) in spring and summer. In the Sea of Japan and the Bay of Biscay (North Spain), solitary and chain forms of *C. tenuissimus* (as *C. salsugineus*) reached important abundances (10^6–10^7 cells l^{-1}) mainly in the summer months (temperature range between 16 and 23°C), but with salinities generally lower than 35 (Orlova & Selina, 1993; Trigueros *et al.*, 2002).

Chaetoceros olympicus

One peculiarity of this new species is the absence of rimoportula both in terminal and in intercalary valves. To our knowledge, the only chain-forming *Chaetoceros* that possesses this feature is the freshwater/brackish species *C. wighamii* Brightwell. As *C. wighamii, C. olympicus* contains a large single chloroplast per cell, their chain apertures are very narrow and their arrangement of setae is similar. However, the cell size is smaller in *C. olympicus* (apical axis between 3.4 and 10.5 µm, Table 2) than in *C. wighamii* (between 14 and 40 µm; Bosak *et al.*, 2015 and references therein). In addition, setae in *C. wighamii* are much stronger and longer and their ultrastructure very different. In *C. wighamii*, the setae show several rows of small poroids arranged in spiral (Bosak *et al.*, 2015) while in *C. olympicus* they present a few slightly twisted rows of small rectangular poroids (Figs 30, 31). Unfortunately, we have not been able to observe the ultrastructure of the valve for *C. olympicus* to compare it with that of *C. wighamii*. The morphological features of *C. olympicus* and *C. wighamii* are summarized in Table 4. Due to its morphological similarity, the marine species *C. bottnicus* Cleve (and the associated species *C. biconcavum* Gran and *C. caspicum* Ostenfeld) was considered by some authors as a synonym of *C. wighamii* but was later reconsidered as a separate species by Sánchez Castillo *et al.* (1992) (see Bosak *et al.*, 2015 for further details). The resting spore of *C. olympicus* is different from that of *C. bottnicus*, whose resting spore is biconvex with spines in one or the two valves (Sánchez Castillo *et al.*, 1992). Therefore, *C. olympicus* cannot be associated with the marine species complex of *C. bottnicus*/*C. biconcavum*/*C. caspicum*.

Apart from strain RCC3007, whose sequence is identical to those of *C. gelidus* and probably corresponds to a misidentification, the sequences obtained in this study were identical to those identified as *C.* cf. *wighamii* from organisms isolated in marine environments. There is no morphological information available for those strains to compare them with the morphological features obtained in this study, but it is unlikely that they correspond to *C. wighamii* as they do not fit with its freshwater ecology. In any case, this highlights the morphological similarity between both species, leading to that labelling of the sequences. An additional sequence identified as *C. wighamii* SAL1 clusters unrelated to the previous sequences and could correspond to the actual *C. wighamii*. Unfortunately, no information about its morphology or isolation source is available to confirm it.

There are some other species, mostly as solitary cells, that lack rimoportula in their valves. These species are *C. subtilis* f. *simplex* Proshkina-Lavrenko, *C. muelleri* var. *subsalsum* (Lemmermann) Johansen & Rushforth, *C. minimus* (Levander) Marino, Giuffre, Montresor & Zingone, *C. transisetus* Johansen & Boyer and *C. coloradensis* Li & Kociolek. All these species differ from the solitary form of *C. olympicus*. *Chaetoceros minimus* has one seta per valve and *C. subtilis* f. *simplex* has the epivalve without setae and one seta in the hypovalve, while *C. olympicus* has 2 setae per each valve. In *C. muelleri* var. *subsalsum* and *C. transisetus* the setae run perpendicular to the pervalvar axis, while in solitary cells of *C. olympicus* setae run at an angle of 45°. In *C. coloradensis*, setae diverge equally from the apical plane as in *C. olympicus* but with a closer angle. In addition, in *C. coloradensis* both valves of the resting spores are smooth while in *C. olympicus* the primary valve is covered with spines.

Other species, mostly lacking ultrastructure observations, present morphological similarities with *C. olympicus*. Morphological characteristics of the morphotype 1 of *C. olympicus* (shape and size of the

Table 4. Morphological characters of *C. olympicus* compared with two similar chain-forming species: *C. tenuissimus* (this study) and *C. wighamii* (Bosak *et al.*, 2015).

Morphological characters	*C. olympicus*	*C. tenuissimus*	*C. wighamii*
Apical axis range (μm)	3.4-5.2 (morph.1), 8.0-10.5 (morph.2)	2.9-6.0	14-26
Life form	Solitary or short-medium size chains	Solitary or short-medium size chains	Usually short chains
Frustules:			
Valve shape	Elliptical	Elliptical	Elliptical
Valve margin	With moderate hyaline rim	With high or low hyaline rim	With high hyaline rim
Mantle	Low	Low	Low
Chloroplast	One	One	One
Aperture	Narrowly lanceolate	Narrowly lanceolate to elliptical	Slit shaped and very narrow
Setae:			
Fusion	At the chain edge	At the chain edge	At the chain edge
Basal part	No	No	No
Divergence from chain axis (Terminal)	Almost at an angle of 45°	In general, at an angle of almost 45°, but it can be variable	U- or V- shaped
Divergence from chain axis (Intercalary)	Perpendicular or slightly oriented towards one end of the chain	Generally, at an angle of almost 45° in the proximal part and perpendicular in the distal part	Variable
Divergence with respect to apical axis	Brunel group II	Brunel group II	Brunel group III (sometimes II)
Cross section	Circular	Circular	Circular
Fine structure and ornamentation	Slightly twisted of few rows of small rectangular poroids and some spines arranged in spiral	Strongly twisted of many rows of small rectangular poroids and several spines arranged in spiral	Longitudinal filaments arranged is spiral interconnected by very short transverse bars forming a spiral row of minute poroids. Helicoidal pattern of spines
Number of poroids in 1 m	16.7 ± 1.1	26.9 ± 1.7	16 (?)
Rimoportula:	Absent	Only in terminal valves	Absent
Number		One	
Location		Centrally	
Shape		Slit	
Resting spores:	Yes	Not observed	Yes
Location	Toward one end of the cell		
Primary valve	Vaulted with short to medium size spines		Valve covered with spines
Secondary valve	Smaller, rounded and smooth		Shaped as a truncated cone

cells/chains, the presence of one chloroplast, the origin and orientation of setae, and resting spore characteristics; Figs 17, 18, 20) match the description of *C.* sp. *B* in Rines & Hargraves (1988) based on light microscopy observations. In turn, these authors mention the similarity of this species with other small chain-forming species such as *C. perpusillus* Cleve, *C. filiformis* Meunier, *C. delicatulus* Ostenfeld, *C. tenuissimus* (as *C. salsugineus* Takano) and *C. muelleri* Lemmermann. However, there is only ultrastructural information available for *C. muelleri* Johansen & Rushforth and *C. tenuissimus*. The distinctive features for the other species are very weak as there is very little information about them. Even so, the morphology of *C. olympicus* observed under LM shows differences with the original descriptions of these species. *Chaetoceros muelleri* was described as solitary or in pairs and possessed a rimoportula in the valve, while *C. olympicus* has no rimoportula. Under light microscopy, the morphotype 1 of *C. olympicus* is very similar to *C. tenuissimus*, both in its solitary and chain forms. Both species are similar in cell size, they have one chloroplast per cell, and their terminal setae have an orientation of 45° with respect to the chain axis. The main differences are the proximal divergence of the intercalary setae (around 45° from chain axis in *C. tenuissimus* and perpendicular or slightly oriented towards one end of the cell in *C. olympicus*) and the observation of resting spores in *C. olympicus* but not in *C. tenuissimus*. The ultrastructure of the cells and setae of both species is also different (Figs 8–16 and 25–32). Table 4 summarizes the mean morphological features of *C. olympicus* and *C. tenuissimus*.

The two morphotypes of *C. olympicus* observed in this study clearly respond to different stages of the life cycle of this species (Figs 33–43). The isolated morphotype (morphotype 1), and therefore the one found in nature, was smaller than morphotype 2 (Table 2). A few days after keeping this species in culture, the formation of an auxospore-like structure was observed in one of the terminal cells of several chains of morphotype 1 (Figs 34–37). It is well known that auxospore formation is the main way that diatoms have for size restitution after their successive mitotic vegetative divisions have reduced cell-size (Mann, 2011). There is a size threshold in which, theoretically, sex is necessary to produce an auxospore, although the environmental conditions or population density may be important factors for sexuality to occur (Mann, 2011). We cannot ensure that the structure that we found corresponds to an auxospore. In fact, no sexual gametes were observed, which does not mean that they were not produced. Anyway, there is evidence that meiosis does not occur in several diatoms and that auxospores are formed asexually or after automixis (Mann, 2011 and references therein). In addition, there are other mechanisms, such as vegetative cell enlargement, by which diatoms can restore their original size. It is possible that the latter mechanism is what occurs in *C. olympicus*.

It seems that, as in *C. tenuissimus*, the solitary form is a life-cycle stage of *C. olympicus*. In nature, an increase in the percentage of solitary cells has been observed after the abundance peak of the chain forms (Table 3). Unfortunately, the *in situ* monitoring of this species was only carried out on morphotype 1, since the existence of morphotype 2 was not known at the time the observations were made. The species was detected in mid-March (late winter), when the study began, but we do not know how long it had been present in the field. However, it seems to be a winter–spring species, since at least its presence as morphotype 1 was detected until May. Further studies are necessary to better understand the dynamics of this species in nature.

Classification of Chaetoceros *in sections – Section* Simplicia

Currently recognized sections are based on morphological information and multigene phylogenies, since phylogenies inferred from single genes do not fully resolve some relationships (De Luca *et al.*, 2019*a*). In this study, the phylogenetic position of studied species was evaluated using SSU and LSU rDNA molecular information separately, in order to determine whether their position agrees using both markers. And in fact, *C. tenuissimus* and *C. olympicus* showed the same phylogenetic position and closest relatives in both phylogenies.

The *Simplicia* section includes species with small, fragile cells, generally solitary or joined in short chains that show no differentiation of terminal setae (Ostenfeld, 1903; De Luca *et al.*, 2019*a*). Up to now, only three species, *C. coloradensis, C. neogracilis, C. tenuissimus*, have been assigned to this section according to the multigene phylogeny of Chaetocerotaceae, since some names from GenBank strains such as *C. muelleri* or *C. calcitrans* are probably uncertain (De Luca *et al.*, 2019*a*). Our emended description of *C. tenuissimus* confirms that the species belonging to section *Simplicia* do not only occur as solitary cells but can form chains within their life cycle. The ability to form colonies was also shown for *C. neogracilis*, which was originally described as a solitary species; thus, this capacity is probably common to other *Chaetoceros* species considered solitary (Balzano *et al.*, 2017).

Chaetoceros olympicus also has the morphological characteristics that define the section *Simplicia*, that is, the species can occur as solitary or colonial forms and has weakly silicified cells, with thin, undifferentiated setae. However, it clustered in a separated and unrelated clade (Figs 44, 45). Interestingly, this clade

is close to the clade representing the section *Minima* in both phylogenies constructed, which includes very small and solitary organisms, characterized by a reduction of the number of setae and with a rimoportula very reduced (in *C. throndsenii*) or absent (in *C. minimus*). Delicate chain-forming organisms with one or two chloroplasts were traditionally assigned to section *Brevicatenata* Gran, although this section is not currently represented in the molecular classification (De Luca *et al.*, 2019*a*). These results confirm that studies on *Chaetoceros* diversity and taxonomy should include both morphological and molecular approaches along with life cycle research, allowing for a more accurate classification of species within the very diverse *Chaetoceros* genus.

Acknowledgements

We are grateful to J.M. Fortuño (Head of the 'Electron and Optical Service' of the Institut de Ciències del Mar (ICM-CSIC) for SEM assistance and SEM microphotography. Inorganic nutrient analyses were performed by M.I. Abad in coordination with E. Berdalet (Head of the Service) at the 'Nutrient Analysis Service' of the ICM-CSIC. We also thank Ll. Cros for the helpful advice on algae culturing and taxonomy and the people involved in the Barcelona samplings. We are also grateful to two anonymous reviewers for helpful comments on the manuscript.

Disclosure statement

No potential conflict of interest was reported by the authors.

Funding

This work was supported by MINECO Project COPAS 'Understanding top-down control in coastal bloom-forming protists' (CTM2017-86121-R), the ANIMA Project (CTM2015-65720-R), and institutional support of the 'Severo Ochoa Centre of Excellence' accreditation (CEX2019-000928-S) from the Spanish government.

Author contributions

L. Arin: original concept, culture establishment, morphological observations, taxonomy, cell counts, drafting and editing the manuscript; A. Reñé: analysis of molecular data, taxonomy, drafting and editing the manuscript; R. Gallisai: analysis of molecular data, review and editing the manuscript; D. Sarno: taxonomy, review and editing the manuscript; E. Garcés: resources, review and editing the manuscript; M. Estrada: resources, review and editing the manuscript.

ORCID

Laura Arin http://orcid.org/0000-0001-8800-5583
Albert Reñé http://orcid.org/0000-0002-0488-3539
Rachele Gallisai http://orcid.org/0000-0003-4224-3265
Diana Sarno http://orcid.org/0000-0001-9697-5301
Esther Garcés http://orcid.org/0000-0002-2712-501X
Marta Estrada http://orcid.org/0000-0001-5769-9498

References

Arin, L., Guillén, J., Segura-Noguera, M. & Estrada, M. (2013). Open sea hydrographic forcing of nutrients and phytoplankton dynamics in a Mediterranean coastal ecosystem. *Estuarine, Coastal and Shelf Science*, **133**: 116–128.

Assmy, P., Hernández-Becerril, D.U. & Montresor, M. (2008). Morphological variability and life cycle traits of the type species of the diatom genus *Chaetoceros, C. dichaeta. Journal of Phycology*, **44**: 152–163.

Balzano, S., Percopo, I., Siano, R., Gourvil, P., Chanoine, M., Marie, D., Vaulot, D. & Sarno, D. (2017). Morphological and genetic diversity of Beaufort Sea diatoms with high contributions from the *Chaetoceros neogracilis* species complex. *Journal of Phycology*, **53**: 161–187.

Baytut, Ö., Moestrup, Ø., Lundholm, N. & Gönülol, A. (2013). Contributions to the diatom flora of the Black Sea from ultrastructural and molecular studies: new records of *Skeletonema marinoi, Pseudo-nitzschia pungens* var. *aveirensis* and *Chaetoceros tenuissimus* for the marine flora of Turkey. *Nova Hedwigia*, **96**: 427–444.

Booth, B.C., Larouche, P., Bélanger, S., Klein, B., Amiel, D. & Mei, Z-P. (2002). Dynamics of *Chaetoceros socialis* blooms in the North Waters. *Deep-Sea Research II*, **49**: 5003–5025.

Bosak, S. (2013). *Taxonomy and ecology of the planktonic diatom family Chaetocerotaceae (Bacillariophyta) from the Adriatic Sea*. Doctoral Thesis, University of Zagreb, 1–256.

Bosak, S., Gligora Udovič, M. & Sarno, D. (2015). Morphological study of *Chaetoceros wighamii* Brightwell (Chaetocerotaceae, Bacillariophyta) from Lake Vrana, Croatia. *Acta Botanica Croatica*, **74**: 233–244.

Bosak, S. & Sarno, D. (2017). The planktonic diatom genus *Chaetoceros* Ehrenberg (Bacillariophyta) from the Adriatic Sea. *Phytotaxa*, **314**: 001–044.

Brunel, J. (1972). Orientation of setae in the genus *Chaetoceros*, in regard to the apical axis. *Journal of the Marine Biological Association of India*, **14**: 315–327.

Capella-Gutiérrez, S., Silla-Martínez, J.M. & Gabaldón, T. (2009). trimAl: a tool for automated alignment trimming in large-scale phylogenetic analyses. *Bioinformatics*, **25**: 1972–1973.

Darriba, D., Taboada, G.L., Doallo, R. & Posada, D. (2012). jModelTest 2: more models, new heuristics and high-performance computing. *Nature Methods*, **9**: 772.

De Luca, D., Sarno, D., Piredda, R. & Kooistra, W.H.C.F. (2019*a*). A multigene phylogeny to infer the evolutionary history of Chaetocerotaceae (Bacillariophyta). *Molecular Phylogenetics Evolution*, **140**: 106575.

De Luca, D., Kooistra, W.H.C.F., Sarno, D., Gaonkar, C.C. & Piredda, R. (2019*b*). Global distribution and diversity of *Chaetoceros* (Bacillariophyta, Mediophyceae):

integration of classical and novel strategies. *PeerJ*. doi: 10.7717/peerj.7410.

Degerlund, M., Huseby, S., Zingone, A., Sarno, D. & Landfald, B. (2012). Functional diversity in cryptic species of *Chaetoceros socialis* Lauder (Bacillariophyceae). *Journal of Plankton Research*, **34**: 416–431.

DeLong, E.F. (1992). Archaea in coastal marine environments. *Proceedings of the National Academy of Sciences USA*, **89**: 5685–5689.

Gaonkar, C.C., Kooistra, W.H.C.F., Lange, C.B., Montresor, M. & Sarno, D. (2017). Two new species in the *Chaetoceros socialis* complex (Bacillariophyta): *C. sporotruncatus* and *C. dichatoensis*, and characterization of its relatives, *C. radicans* and *C. cinctus*. *Journal of Phycology*, **53**: 889–907.

Gaonkar, C.C., Piredda, R., Minucci, C., Mann, D.G., Montresor, M., Sarno, D. & Kooistra, W.H.C.F. (2018). Annotated 18S and 28S rDNA reference sequences of taxa in the planktonic diatom family Chaetocerotaceae. *PLoS ONE*, **13**: e0208929.

Grasshoff, K., Kremling, K. & Ehrhardt, M. (1999). *Methods of Seawater Analysis*. Verlag Wiley-VCH, Weinheim.

Guerrero, E., Abelló, P., Lombarte, A., Villanueva, R., Ramón, M., Sabatés, A. & Santos, R. (2020). *Biological Reference Collections ICM-CSIC*. v1.28. Institute of Marine Sciences (ICM-CSIC). Dataset/Occurrence. https://doi.org/10.15470/qlqqdx.

Guiry, M.D. & Guiry, G.M. (2021). *AlgaeBase*. World-wide electronic publication, National University of Ireland, Galway. http://www.algaebase.org.

Hasle, G.R. & Syvertsen, E.S. (1997). Marine diatoms. In *Identifying Marine Phytoplankton* (Tomas, C.R., editor). Academic Press, London.

Hernández-Becerril, D.U. (1991). The morphology and taxonomy of the planktonic diatom *Chaetoceros coarctatus* Lauder (Bacillariophyceae). *Diatom Research*, **6**: 281–287.

Hernández-Becerril, D.U. (1996). A morphological study of *Chaetoceros* species (Bacillariophyta) from the plankton of the Pacific Ocean of Mexico. *Bulletin of the Natural History Museum of London*, **26**: 1–73.

Hernández-Becerril, D.U. & Flores Granados, C. (1998). Species of the diatom genus *Chaetoceros* (Bacillariophyceae) in the plankton from the southern Gulf of Mexico. *Botanica Marina*, **41**: 505–519.

Hoppenrath, M., Elbrächter, M. & Drebes, G. (2009). *Marine Phytoplankton: Selected Microphytoplankton Species from the North Sea around Helgoland and Sylt*. E. Schweizerbart Science Publishers, Stuttgart.

Horner, R.A., Garrison, D.L. & Plumley, F.G. (1997). Harmful algal blooms and red tide problems on the U.S. west coast. *Limnology and Oceanography*, **45**: 1076–1088.

Ichimi, K., Kawamura, T., Yamamoto, A., Tada, K. & Harrison, P.J. (2012). Extremely high growth rate of the small diatom *Chaetoceros salsugineus* isolated from an estuary in the eastern Seto Inland Sea, Japan. *Journal of Phycology*, **48**: 1284–1288.

Katoh, K., Rozewicki, J. & Yamada, K.D. (2019). MAFFT online service: multiple sequence alignment, interactive sequence choice and visualization. *Briefings in Bioinformatics*, **20**: 1160–1166.

Kooistra, W.H.C.F., Sarno, D., Hernández-Becerril, D.U., Assmy, P., Di Prisco, C. & Montresor, M. (2010). Comparative molecular and morphological phylogenetic analyses of taxa in the *Chaetocerotaceae* (Bacillariophyta). *Phycologia*, **49**: 471–500.

Li, Y., Boonprakob, A., Gaonkar, C.C., Kooistra, W.H.C.F., Lange, C.B., Hernández-Becerril, D., Chen, Z., Moestrup, Ø. & Lundholm, N. (2017). Diversity in the globally distributed diatom genus *Chaetoceros* (Bacillariophyceae): three new species from warm-temperate waters. *PLoS ONE*, **12**: e0168887.

Li, Y., Zhu, S., Lundholm, N. & Lü, S. (2015) Morphology and molecular phylogeny of *Chaetoceros dayaensis* sp. nov. (Bacillariophyceae), characterized by two 90o rotations of the resting spore during maturation. *Journal of Phycology*, **51**: 469–479.

Malviya, S., Scalco, E., Audic, S., Vincent, F., Veluchamy, A., Poulain, J., Wincker, P., Iudicone, D., de Vargas, C., Bittner, L., Zingone, A. & Bowler, C. (2016). Insights into global diatom distribution and diversity in the world's ocean. *Proceedings of the National Academy of Sciences USA*, **113**: E1516–E1525.

Mann, D.G. (2011). Size and sex. In *The Diatom World* (Seckbach, J. & Kociolek, J.P., editors). Springer, Cham.

Medlin, L., Elwood, H.J., Stickel, S. & Sogin, M.L. (1988). The characterization of enzymatically amplified eukaryotic 16S-like rRNA-coding regions. *Gene*, **71**: 491–499.

Meunier, A. (1913). Microplankton de la Mer Flamande. 1ère Partie. Le genre *Chaetoceros* Ehr. *Mémoires du Musée Royal d'Histoire Naturelle de Belgique*, **7**: 1–58.

Nunn, G.B., Theisen, B.F., Christensen, B. & Arctander, P. (1996). Simplicity-correlated size growth of the nuclear 28S ribosomal RNA D3 expansion segment in the crustacean order Isopoda. *Journal of Molecular Evolution*, **42**: 211–223.

Orlova, T.Y. & Aizdaicher, N.A. (2000). Development in culture of the diatom *Chaetoceros salsugineus* from the Sea of Japan. *Russian Journal of Marine Biology*, **26**: 8–11.

Orlova, T.Y. & Selina, M.S. (1993). Morphology and ecology of the bloom-forming planktonic diatom *Chaetoceros salsugineus* Takano in the Sea of Japan. *Botanica Marina*, **36**: 123–130.

Ostenfeld, C.H. (1903). Plankton from the sea around the Færöes. In *Botany of the Færöes* (Warming, E., editor). Nordisk Forlag, Copenhagen.

Ribera D'Alcalà, M., Conversano, F., Corato, F., Licandro, P., Mangoni, O., Marino, D., Mazzocchi, M.G., Modigh, M., Montresor, M., Nardella, M., Saggiomo, V., Sarno, D. & Zingone, A. (2004) Seasonal patterns in plankton communities in a pluriannual time series at a coastal Mediterranean site (Gulf of Naples): an attempt to discern recurrences and trends. *Scientia Marina*, **68**(**SI**): 65–83.

Rines, J.E.B. & Hargraves, P.E. (1988). *The* Chaetoceros *Ehrenberg (Bacillariophyceae) Flora of Narragansett Bay, Rhode Island, USA*. Bibliotheca Phycologica, Berlin.

Rines, J.E.B. & Theriot, E.C. (2003). Systematics of Chaetocerotaceae (Bacillariophyceae). I. A phylogenetic analysis of the family. *Phycological Research*, **51**: 83–98.

Ronquist, F., Teslenko, M., Van Der Mark, P., Ayres, D.L., Darling, A., Höhna, S., Larget, B., Liu, L., Suchard, M.A. & Huelsenbeck, J.P. (2012). MrBayes 3.2: Efficient Bayesian Phylogenetic Inference and Model Choice across a Large Model Space. *Systematic Biology*, **61**: 539–542.

Sánchez Castillo, P.M., Ubierna Leon, M.A. & Round, F.E. (1992). Estudio de *Chaetoceros wighamii* Brightwell: un taxon mal interpretado. *Diatom Research*, **22**: 441–448.

Sar, E.A., Hernández-Becerril, D.U. & Sunesen, I. (2002). A morphological study of *Chaetoceros tenuissimus* Meunier, a little-known planktonic diatom, with a discussion of the section *Simplicia*, subgenus Hyalochaete. *Diatom Research*, **17**: 327–335.

Scholin, C.A., Herzog, M., Sogin, M. & Anderson, D.M. (1994) Identification of group- and strain-specific genetic markers for globally distributed *Alexandrium* (Dinophyceae). II. Sequence analysis of a fragment of the LSU rRNA gene. *Journal of Phycology*, **30**: 999–1011.

Shevchenko, O.G. & Orlova, T.Y. (2010). Morphology and ecology of the bloom-forming diatom *Chaetoceros contortus* from Peter the Great Bay, Sea of Japan. *Russian Journal of Marine Biology*, **36**: 243–251.

Shevchenko, O.G., Orlova, T.Y. & Hernández-Becerril, D. U. (2006). The genus *Chaetoceros* (Bacillariophyta) from Peter the Great Bay, Sea of Japan. *Botanica Marina*, **49**: 236–258.

Stamatakis, A. (2014). RAxML version 8: a tool for phylogenetic analysis and post-analysis of large phylogenies. *Bioinformatics*, **30**: 1312–1313.

Takano, H. (1983). New and rare diatoms from Japanese marine waters. X. A new *Chaetoceros* common in estuaries. *Bulletin of Tokai Regional Fisheries Research Laboratory*, **110**: 1–11.

Throndsen, J. (1978). Preservation and storage. In *Phytoplankton Manual* (Sournia, A. editor), 69–74. UNESCO, Paris.

Tomaru, Y., Toyoda, K. & Kimura, K. (2018). Occurrence of the planktonic bloom-forming marine diatom *Chaetoceros tenuissimus* Meunier and its infectious viruses in western Japan. *Hydrobiologia*, **805**: 221–230.

Treasurer, J.W., Hannah, F. & Cox, D. (2003). Impact of a phytoplankton bloom on mortalities and feeding response of framed Atlantic salmon, *Salmo salar*, in west Scotland. *Aquaculture*, **218**: 103–113.

Trigueros, J.M., Orive, E. & Arriluzea, J. (2002). Observations on *Chaetoceros salsugineus* (Chaetocerotales, Bacillario phyceae): first record of this bloom-forming diatom in a European estuary. *European Journal of Phycology*, **37**: 571–578.

Utermöhl, H. (1958). Zur Vervollkommung der quantitativen Phytoplankton-Methodik. *Mitteilungen. Internationale Vereiningung fuer Theoretische und Angewandte Limnologie*, **9**: 1–38.

Yentsch, C.S. & Menzel, D.W. (1963). A method for the determination of phytoplankton chlorophyll and phaeophytin by fluorescence. *Deep-Sea Research*, **10**: 221–231.